LECTURE NOTES

Non-equilibrium phase transitions

Haye Hinrichsen

Fakultät für Physik und Astronomie, Universität Würzburg,
D–97074 Würzburg, Germany

E-mail: hinrichsen@physik.uni-wuerzburg.de

Lectures held at the
International Summer School on
Problems in Statistical Physics XI

Leuven, Belgium, September 2005

Abstract: These lecture notes give a basic introduction to the physics of phase transitions under non-equilibrium conditions. The notes start with a general introduction to non-equilibrium statistical mechanics followed by four parts. The first one discusses the universality class of directed percolation, which plays a similar role as the Ising model in equilibrium statistical physics. The second one gives an overview about other universality classes which have been of interest in recent years. The third part extends the scope to models with long-range interactions, including memory effects and so-called Lévy flights. Finally, the fourth part is concerned with deposition-evaporation phenomena leading to wetting transitions out of equilibrium.

Contents

1. Introduction

This lecture is concerned with classical stochastic many-particle systems far away from thermal equilibrium. Such systems are used as models of a much more complex physical reality with many degrees of freedom in which chaotic or quantum-mechanical effects lead effectively to a classical random dynamics on a coarse-grained scale.

In order to explain the notion of stochastic non-equilibrium systems, let us for example consider an experimental setup of molecular beam epitaxy. On a fundamental level a freshly deposited diffusing atom is described by a quantum-mechanical wave function that evolves under the influence of various interactions with the substrate and the environment. However, monitoring the particle by modern imaging techniques, it seems to behave as a classical object that hops occasionally from one lattice site to the other. In fact, in contrast to isolated quantum-mechanical particles, whose wave packages spread in time, the deposited atom is exposed to a complex variety of interactions and entanglements with the environment which lead to a continuous *decoherence* of the quantum state [1]. This process of decoherence keeps the wave package localized and thereby pinned to a certain lattice site as time proceeds. The opposing quantum effect of *recoherence*, however, leads to occasional tunneling through the surrounding energy barriers. Immediately after tunneling, decoherence again localizes the wave function at the target site, destroying all information encoded in quantum-mechanical phases. This means that several subsequent tunneling events are effectively uncorrelated, provided that they are separated by time intervals that are much larger than the typical decoherence time. It is this separation of time scales that allows one to consider the particle as a classical object that evolves in time by spontaneous uncorrelated random moves to neighboring sites. Using this classical picture it is no longer necessary to consider the full wave function of the particle, rather it is sufficient to characterize its state by the index of the lattice site to which it is pinned at time t and the effective transition rates by which it hops to its nearest neighbors. This interpretation can be extended to chemical reactions as well.

1.1. Master equation

More generally, a classical stochastic many-particle system is defined by a set C of possible configurations of the particles $c \in C$. The process evolves in time by instantaneous transitions $c \to c'$ which occur spontaneously like in a radioactive decay with certain rates $w_{c\to c'} \geq 0$. The set of all configurations, the transition rates and the initial state fully define the stochastic model under consideration.

From the theoretical point of view an important object to study is the probability $P_t(c)$ to find the system at time t in a certain configuration c. Obviously this probability distribution has to be normalized, i.e., $\sum_c P_t(c) = 1$. While the evolution of the system's configuration is generally unpredictable due to its stochastic nature, the temporal evolution of the probability distribution $P_t(c)$ *is* predictable and given by a linear system of differential equations. This system of equations, usually called *master equation*, describes the flow of probability between different configurations in terms of gain and

loss contributions:

$$\frac{\partial}{\partial t}P_t(c) = \underbrace{\sum_{c'} w_{c'\to c}P_t(c')}_{\text{gain}} - \underbrace{\sum_{c'} w_{c\to c'}P_t(c)}_{\text{loss}} \ . \tag{1}$$

The gain and loss terms balance one another so that the probability distribution remains normalized as time proceeds. It is important to note that the coefficients $w_{c\to c'}$ are *rates* rather than probabilities and carry the unit $[\text{time}]^{-1}$. Therefore, rates may be larger than 1 and can be rescaled by changing the time scale.

In a more compact form this set of equation may be written as

$$\partial_t|P_t\rangle = -\mathcal{L}|P_t\rangle \ , \tag{2}$$

where $|P_t\rangle$ denotes a vector whose entries are the probabilities $P_t(c)$. This means that the corresponding vector space has a dimension equal to the number of possible configurations. The so-called Liouville operator $\mathcal{L}$ generates the temporal evolution and is defined in the canonical configuration basis by the matrix elements

$$\langle c'|\mathcal{L}|c\rangle = -w_{c\to c'} + \delta_{c,c'}\sum_{c''} w_{c\to c''}. \tag{3}$$

A formal solution of this first-order differential equation is given by $|P_t\rangle = \exp(-\mathcal{L}t)|P_0\rangle$, where $|P_0\rangle$ denotes the initial probability distribution at $t = 0$. This means that $|P_t\rangle$ can be expressed as a sum over exponentially varying eigenmodes.

Since most stochastic processes are irreversible and therefore not invariant under time reversal, the Liouville operator $\mathcal{L}$ is generally non-hermitean. However, the form of $\mathcal{L}$ is restricted by the requirements of the aforementioned balance between gain and loss terms as well as by the positivity of the rates. In the mathematical literature such matrices are usually called *intensity matrices*, meaning that all diagonal (off-diagonal) entries are real and positive (negative) and that the sum over each column of the matrix vanishes. The eigenvalues of an intensity matrix may be complex, indicating oscillatory behavior, but their real part is always non-negative. Moreover, probability conservation ensures that the spectrum includes at least one zero mode $\mathcal{L}|P_s\rangle = 0$, representing the stationary probability distribution of the system. The other eigenvalues with positive real parts represent relaxational eigenmodes which decay exponentially with time. Therefore, if all other eigenvalues have strictly positive real parts, a stochastic process with a finite configuration space approaches a well-defined stationary probability distribution $P_\infty(c)$ exponentially.

1.2. Equilibrium dynamics

Equilibrium statistical mechanics is based on the axiom that the underlying quantum-mechanical laws are built in such a way that an *isolated* stochastic system in its stationary state maximizes entropy. This means that it evolves through the accessible configurations with the same probability, forming a microcanonical ensemble. In most applications, however, the stochastic system is not isolated but coupled to an external

heat bath. A heat bath is a surrounding environment consisting of many degrees of freedom that exchanges energy with the system of interest. For example, in molecular beam epitaxy the deposited particle interacts with the phonons of the substrate by an exchange of energy, i.e., the substrate provides a thermal heat bath. Assuming that the combination of system and heat bath maximizes entropy while conserving energy it is easy to show that the stationary probability distribution $P_{eq}(c)$ is no longer uniform but given by the Boltzmann ensemble

$$P_{eq}(c) = \frac{1}{Z} \exp(-E(c)/k_B T)\,, \tag{4}$$

where T is the temperature of the heat bath and Z is the partition sum over all accessible configurations. Therefore, in equilibrium statistical mechanics it is not necessary to solve a partial differential equation, instead the stationary distribution is delivered for free.

Equilibrium models are fully defined by the accessible configurations $c \in C$ and the corresponding energies $E(c)$. Although the Boltzmann ensemble renders the stationary distribution for free it does not provide any information about relaxational modes. Consequently, the dynamical rules for a given equilibrium system in terms of transition rates are not unique. In fact, as the only requirement the stationary zero mode of the Liouville operator has to reproduce the Boltzmann ensemble, which determines the matrix elements of $\mathcal{L}$ only partially. This is the reason why the well-known Ising model can be simulated on a computer by various dynamical algorithms, including heat bath, Glauber, Metropolis, and Swendsen-Wang dynamics. All these dynamical processes relax towards the same stationary state that reproduces the Boltzmann ensemble of the Ising model. However, their dynamical properties can be quite different which plays an important role with respect to critical slowing down in the vicinity of a phase transition.

Constructing dynamical rules that reproduce the stationary distribution of a given equilibrium model, it is always possible to choose the transition rates in such a way that they obey *detailed balance*, i.e.

$$P_{eq}(c)\, w_{c\to c'} \;=\; P_{eq}(c')\, w_{c'\to c}\;. \tag{5}$$

This means that the probability currents between pairs of configurations c and c' cancel each other, as sketched in the left panel of Fig. 1.

1.3. Non-equilibrium dynamics

Dynamical systems are said to be out of equilibrium if the microscopic processes violate detailed balance. Roughly speaking, the term "non-equilibrium" refers to situations where the probability currents between microstates do not vanish. For example, an Glauber-Ising model that has not yet reached the stationary state violates detailed balance and hence is out of equilibrium. But even systems in a stationary state can be out of equilibrium. Let us, for example, consider a system with three configurations A, B, C that hops clockwise by cyclic transition rates $w_{A\to B} = w_{B\to C} = w_{C\to A} = 1$ (see right panel of Fig. 1). This process quickly approaches a stationary state with equal probabilities $P_s(A) = P_s(B) = P_s(C) = 1/3$. Although this stationary distribution

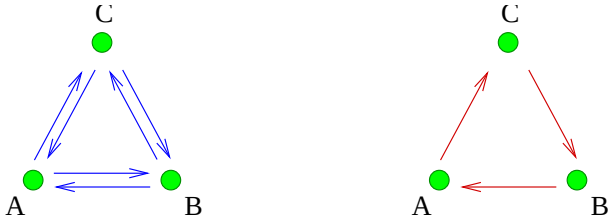

Figure 1. Detailed balance and non-equilibrium steady states. The figure sketches a hypothetical system with three microstates A, B, C. In both cases the stationary distribution function is $P_s(A) = P_s(B) = P_s(C) = 1/3$. Left: The transitions occur at equal rates in all directions, hence the effective probability currents vanish and the dynamics obeys detailed balance. Right: The transitions occur only clockwise, leading to non-vanishing probability currents. Consequently, even the stationary state of the system is out of equilibrium.

corresponds to a Boltzmann distribution with constant energy, the process violates the condition of detailed balance and is therfore out of equilibrium.

On a more hand-waving level all systems subjected to external currents such as external driving or supply of energy or particles are expected to be out of equilibrium. For example, a running steam engine, although working in a stationary situation, needs continuous supply of air, coal, and water, hence it is in principle impossible to establish detailed balance. Nevertheless a steam engine is still close to equilibrium, meaning that on certain scales the processes are almost thermalized so that the concepts of equilibrium physics can still be applied.

In this lecture, we are primarily interested in systems *far* from equilibrium. To this end we consider stochastic processes that violate detailed balance so strongly that concepts of equilibrium statistical physics can no longer be applied, even in an approximate sense. We are interested in the question whether stochastic processes far from equilibrium can exhibit new phenomena that cannot be observed under equilibrium conditions. This applies in particular to *phase transitions* far from equilibrium.

1.4. Non-equilibrium phase transitions

Particularly interesting in classical stochastic systems are situations in which the microscopic degrees of freedom behave collectively over large scales [2,3], especially when the system undergoes a continuous phase transition. In equilibrium statistical mechanics the best known example is the order-disorder transition in the two-dimensional Ising model, where the typical size of ordered domains diverges when the critical temperature T_c is approached. It is well known that in second-order phase transition at thermal equilibrium the emerging long-range correlations are fully specified by the symmetry properties of the model under consideration and do not depend on details of the microscopic interactions. This allows one to associate these transitions with different *universality classes*. The notion of universality was originally introduced by experimentalists in order to describe the observation that several apparently unrelated physical systems are sometimes characterized by the same type of singular behavior near the transition. Since then the concept of universality classes became a paradigm

of statistical physics. As the number of such classes seems to be limited, the aim of theoretical statistical mechanics would be to provide a complete classification scheme. The most remarkable breakthrough in this direction was the application of conformal field theory to equilibrium critical phenomena [4–6], leading to an extremely powerful classification scheme of continuous phase transitions in two dimensions.

Continuous phase transitions far away from equilibrium are less well understood. It turns out that the concept of *universality*, which has been very successful in the field of equilibrium critical phenomena, can be applied to non-equilibrium phase transitions as well. However, the universality classes of non-equilibrium critical phenomena are expected to be even more diverse as they involve time as an extra degree of freedom and are therefore governed by various symmetry properties of the evolution dynamics. Obviously, there is a large variety of phenomenological non-equilibrium phase transitions in Nature, ranging for example from morphological transitions of growing surfaces [7] to traffic jams [8]. On the other hand, the experimental evidence for universality of non-equilibrium phase transitions is still very poor, calling for intensified experimental efforts.

One important class of non-equilibrium phase transitions, on which we will focus in this lecture, occurs in models with so-called absorbing states, i.e., configurations that can be reached by the dynamics but cannot be left. The most prominent universality class of absorbing-state transitions is *directed percolation* (DP) [9]. This type of transition occurs, for example, in models for the spreading of infectious diseases. Amazingly, DP is one of very few critical phenomena which cannot be solved exactly in one spatial dimension. Although DP is easy to define, its critical behavior is highly nontrivial. This is probably one of the reasons why DP keeps theoretical physicists fascinated.

Moreover, these lecture notes discuss various other classes of non-equilibrium phase transitions and give a short introduction to wetting far from equilibrium. The presentation is based on various existing sources, in particular on the book by Marro and Dickman [10] and the review articles by Kinzel [9], Grassberger [11], Ódor [12], Lübeck [13], and myself [14]. The reader is also referred to a large number of research articles for further reading.

2. Directed percolation

The probably most important class of non-equilibrium processes, which display a non-trivial phase transition from a fluctuating phase into an absorbing state, is *Directed Percolation* (DP). As will be discussed below, the DP class comprises a large variety of models that share certain basic properties.

2.1. Directed bond percolation on a lattice

To start with let us first consider a specific model called *directed bond percolation* which is often used as a simple model for water percolating through a porous medium. The model is defined on a tilted square lattice whose sites represent the pores of the medium. The pores are connected by small channels (bonds) which are open with probability p and closed otherwise. As shown in Fig. 2, water injected into one of the pores will

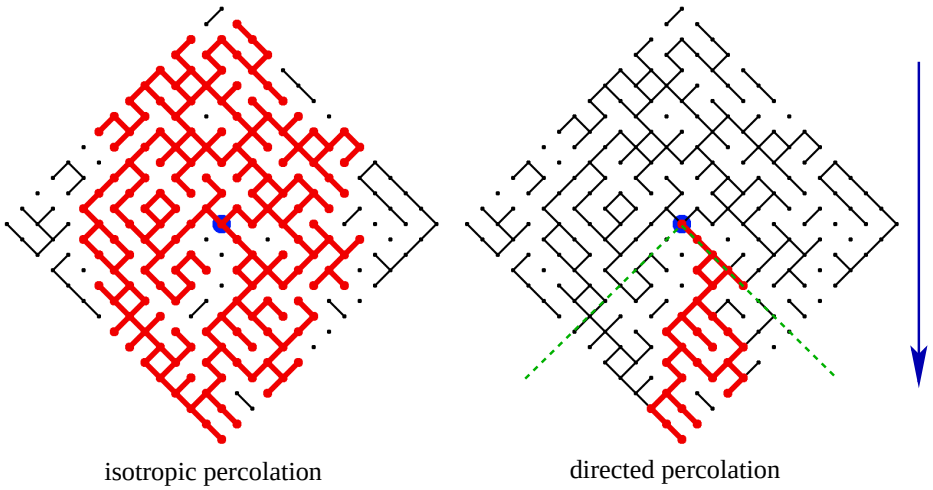

Figure 2. Isotropic versus directed bond percolation. The figure shows two identical realizations of open and closed bonds on a finite part of a tilted square lattice. A spreading agent (red) is injected at the central site (blue circle). In the case of isotropic percolation (left) the agent percolates through open bonds in any direction. Contrarily, in the case of directed percolation, the agent is restricted to percolate along a preferred direction, as indicated by the arrow.

percolate along open channels, giving rise to a percolation cluster of wetted pores whose average size will depend on p.

There are two fundamentally different versions of percolation models. In *isotropic percolation* the flow is undirected, i.e., the spreading agent (water) can flow in any direction through open bonds (left panel of Fig. 2). A comprehensive introduction to isotropic percolation is given in the textbook by Stauffer [15]. In the present lecture, however, we are primarily interested in the case of *directed* percolation. Here the clusters are directed, i.e., the water is restricted to flow along a preferred direction in space, as indicated by the arrow in Fig. 2. In the context of porous media this preferred direction may be interpreted as a gravitational driving force. Using the language of electronic circuits DP may be realized as a random diode network (cf. Sect. 2.9).

The strict order of cause and effect in DP allows one to interpret the preferred direction as a temporal coordinate. For example, in directed bond percolation, we may enumerate horizontal rows of sites by an integer time index t (see Fig. 3). Instead of a static model of directed connectivity, we shall from now on interpret DP as a dynamical process which evolves in time. Denoting wetted sites as *active* and dry sites as *inactive* the process starts with a certain initial configuration of active sites that can be chosen freely. For example, in Fig. 3 the process starts with a single active seed at the origin. As t increases the process evolves stochastically through a sequence of configurations of active sites, also called *states* at time t. An important quantity, which characterizes these intermediate states, is the total number of active sites $N(t)$, as illustrated in Fig. 3.

Regarding directed percolation as a reaction-diffusion process the local transition rules may be interpreted as follows. Each active site represents a particle A. If the two subsequent bonds are both closed, the particle will have disappeared at the next time step by a death process $A \to \emptyset$ (see Fig. 4a). If only one of the bonds is open,

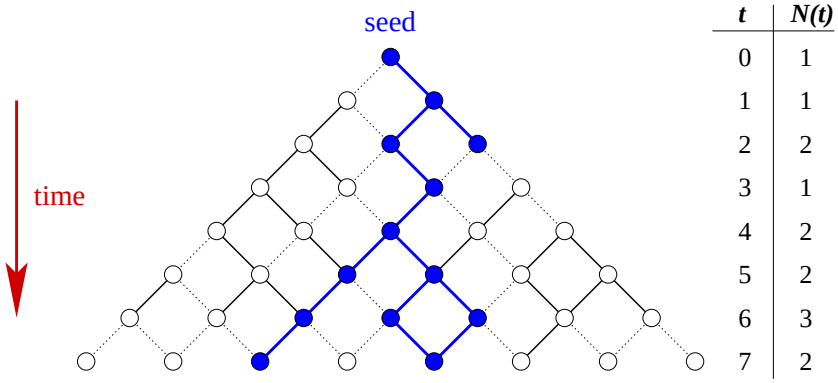

Figure 3. Directed bond percolation. The process shown here starts with a single active seed at the origin. It then evolves through a sequence of configurations along horizontal lines (called states) which can be labeled by a time-like index t. An important quantity to study would be the total number of active sites $N(t)$ at time t.

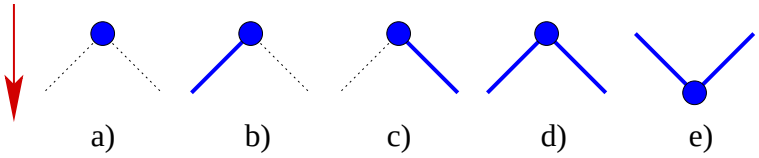

Figure 4. Interpretation of the dynamical rules of directed bond percolation as a reaction-diffusion process: a) death process, b)-c) diffusion, d) offspring production, and e) coagulation.

the particle diffuses stochastically to the left or to the right, as shown in Fig. 4b-4c. Finally, if the two bonds are open the particles creates an offspring $A \to 2A$ (Fig. 4d). However, it is important to note that each site in directed bond percolation can be either active or inactive. In the particle language this means that each site can be occupied by at most one particle. Consequently, if two particles happen to reach the same site, they merge irreversibly forming a single one by coalescence $2A \to A$, as illustrated in Fig. 4e. Summarizing these reactions, directed bond percolation can be interpreted as a reaction-diffusion process which effectively follows the reaction scheme

$$\begin{array}{ll} A \to \emptyset & \text{death process} \\ A \to 2A & \text{offspring production} \\ 2A \to A & \text{coagulation} \end{array} \qquad (6)$$

combined with single-particle diffusion.

The dynamical interpretation in terms of particles is of course the natural language for any algorithmic implementation of DP on a computer. As the configuration at time t depends exclusively on the previous configuration at time $t-1$ it is not necessary to store the entire cluster in the memory, instead it suffices to keep track of the actual configuration of active sites at a given time and to update this configuration in parallel sweeps according to certain probabilistic rules. In the case of directed bond percolation, one obtains a stochastic cellular automaton with certain update rules in which each active site of the previous configuration activates its nearest neighbors of the actual configuration with probability p. In fact, as shown in Fig. 5, a simple non-optimized

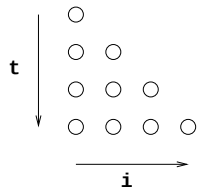


```
//============== Simple C-code for directed percolation =============

#include <fstream.h>
using namespace std;

const int T=1000;                // number of rows
const int R=10000;               // number of runs
const double p=0.7;              // percolation probability
int N[T];                        // cumulative occupation number

//--- random number generator returning doubles between 0 and 1 -----

inline double rnd(void) { return (double)rand()/0x7FFFFFFF; }

//------------ construct directed percolation cluster ---------------

void DP (void)  {
int t,i,s[T][T];                                    // static array
for (t=0;t<T;t++) for (i=0;i<=t;i++) s[t][i]=0;  // clear lattice
s[0][0]=1;                                          // place seed
// perform loop over all active sites:
for (t=0; t<T-1; t++) for (i=0; i<=t; i++) if (s[t][i]) {
        N[t]++;
        if (rnd()<p) s[t+1][i]=1;               // offspring right
        if (rnd()<p) s[t+1][i+1]=1;             // offspring left
        }
}

//-------- perform R runs and write average N(t) to disk -----------

int main (void) {
for (int t=0; t<T; t++) N[t]=0;          // reset N(t)
for (int r=0; r<R; r++) DP();            // perform R runs
ofstream os("N.dat");                    // write result to disk
for (int t=0; t<T-1; t++) os << t << "\t" << (double)N[t]/R << endl;
}
```

Figure 5. Simple non-optimized program in C for directed bond percolation. The numerical results are shown below in Fig. 6.

C-code for directed bond percolation takes less than a page, and the core of the update rules takes only a few lines.

2.2. Absorbing states and critical behavior

As only active sites at time t can activate sites at time $t+1$, the configuration *without* active sites plays a special role. Obviously, such a state can be reached by the dynamics but it cannot be left. In the literature such states are referred to as *absorbing*. Absorbing

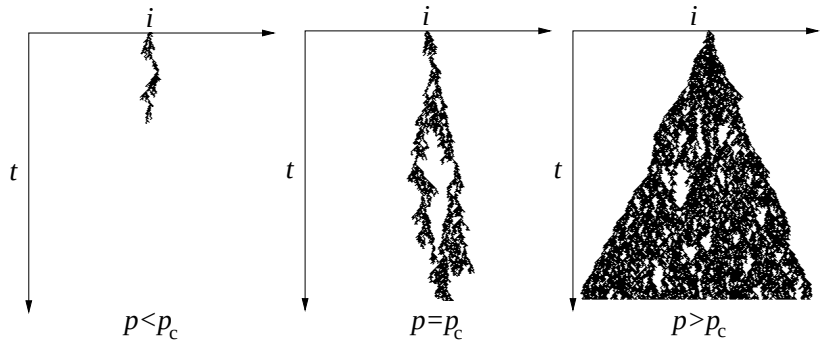

Figure 6. Typical DP clusters in 1+1 dimensions grown from a single seed below, at, and above criticality.

states can be thought of as a trap: Once the system reaches the absorbing state it becomes trapped and will stay there forever. As we will see below, a key feature of directed percolation is the presence of a *single* absorbing state, usually represented by the empty lattice.

The mere existence of an absorbing state demonstrates that DP is a dynamical process far from thermal equilibrium. As explained in the Introduction, equilibrium statistical mechanics deals with stationary equilibrium ensembles that can be generated by a dynamics obeying detailed balance, meaning that probability currents between pairs of sites cancel each other. As the absorbing state can only be reached but not be left, there is always a non-zero current of probability into the absorbing state that violates detailed balance. Consequently the temporal evolution before reaching the absorbing state cannot be described in terms of thermodynamic ensembles, proving that DP is a non-equilibrium process.

The enormous theoretical interest in DP – more than 800 articles refer to this class of models – is related to the fact that DP displays a *non-equilibrium phase transition* from a fluctuating phase into the absorbing state controlled by the percolation probability p. The existence of such a transition is quite plausible since offspring production and particle death compete with each other. As will be discussed below, phase transitions into absorbing states can be characterized by certain *universal properties* which are independent of specific details of the microscopic dynamics. In fact, the term 'directed percolation' does not stand for a particular model, rather it denotes a whole universality class of models which display the same type of critical behavior at the phase transition. The situation is similar as in equilibrium statistical mechanics, where for example the Ising universality class comprises a large variety of different models. In fact, DP is probably as fundamental in non-equilibrium statistical physics as the Ising model in equilibrium statistical mechanics.

In DP the phase transition takes place at a certain well-defined critical percolation probability p_c. As illustrated in Fig. 6 the behavior on both sides of p_c is very different. In the subcritical regime $p < p_c$ any cluster generated from a single seed has a finite life time and thus a finite mass. Contrarily, in the supercritical regime $p > p_c$ there is a finite probability that the generated cluster extends to infinity, spreading roughly within a cone whose opening angle depends on $p-p_c$. Finally, at criticality finite clusters of all sizes are generated. These clusters are sparse and remind of self-similar fractal

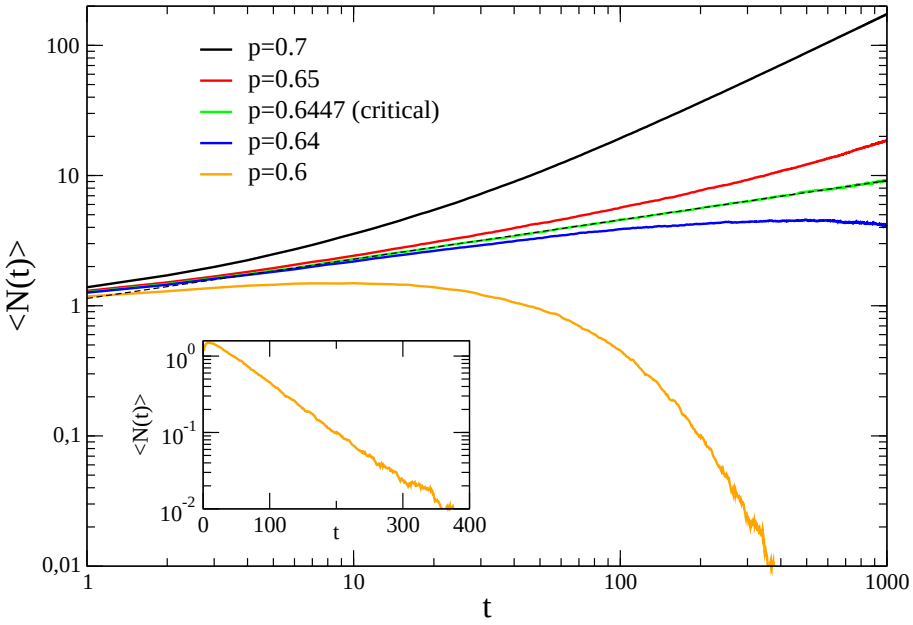

Figure 7. Directed bond percolation: Number of particles $N(t)$ as a function of time for different values of the percolation probability p. The critical point is characterized by an asymptotic power law behavior. The inset demonstrates the crossover to an exponential decay in the subcritical phase for $p = 0.6$.

objects. As we will see, a hallmark of such a scale-free behavior is a power-law behavior of various quantities.

The precise value of the percolation threshold p_c is non-universal (i.e., it depends on the specific model) and can only be determined numerically. For example, in the case of directed bond percolation in 1+1 dimensions, the best estimate is $p_c = 0.644700185(5)$ [16]. Unlike isotropic bond percolation in two dimensions, where the critical value is exactly given by $p_c^{\rm iso} = 1/2$, an analytical expression for the critical threshold of DP in finite dimensions is not yet known. This seems to be related to the fact that DP is a non-integrable process. It is in fact amazing that so far, in spite of its simplicity and the enormous effort by many scientists, DP resisted all attempts to be solved exactly, even in 1+1 dimensions.

In order to describe the phase transition quantatively an appropriate order parameter is needed. For simulations starting from a single active seed a suitable order parameter is the average number of particles $\langle N(t)\rangle$ at time t, where $\langle \ldots \rangle$ denotes the average over many independent realizations of randomness (called *runs* in the numerical jargon). For example, the program shown in Fig. 5 averages this quantity over 10.000 runs and stores the result in a file that can be viewed by a graphical tool such as `xmgrace`. As shown in Fig. 7, there are three different cases:

- For $p < p_c$ the average number of active sites first increases and then decreases rapidly. As demonstrated in the inset, this decrease is in fact exponential. Obviously, the typical crossover time, where exponential decay starts, depends on the distance from criticality $p_c - p$.

- At criticality the average number of active sites increases according to a power law $\langle N(t)\rangle \sim t^{\theta}$. A standard regression of the data gives the exponent $\theta \simeq 0.302$, shown in the figure as a thin dashed line. As can be seen, there are deviations for low t, i.e., the process approaches a power-law only asymptotically.

- In the supercritical regime $p > p_c$ the slow increase of $\langle N(t)\rangle$ crosses over to a fast linear increase with time. Again the crossover time depends on the distance from criticality $p - p_c$.

The properties of $\langle N(t)\rangle$ above and below criticality can be used to determine the critical threshold numerically. This iterative procedure works as follows: Starting with a moderate simulation time it is easy to specify a lower and an upper bound for p_c by hand, e.g., $0.64 < p_c < 0.65$ in the case of directed bond percolation. This interval is then divided into two equal parts and the process is simulated in between, e.g., at $p = 0.645$. In order to find out whether this value is sub- or supercritical one has to check deviations for large t from a straight line in a double logarithmic plot. If the curve veers down (up) the procedure is iterated using the upper (lower) interval. In detecting the sign of curvature the human eye is quite reliable but it is also possible to recognize it automatically. If there is no obvious deviation from a straight line the simulation time and the number of runs has to be increased appropriately.

Warning: Determining the numerical error for the estimate of a critical exponent never use the statistical χ^2-error of a standard regression! For example, for the data produced by the minimal program discussed above, a linear regression by `xmgrace` would give the result $\theta = 0.3017(2)$. However, the estimate in the literature $\theta = 0.313686(8)$ lies clearly outside these error margins, meaning that the actual error must be much higher. A reliable estimate of the error can be obtained by comparing the slopes over the last decade of simulations performed at the upper and the lower bound of p_c.

In principle the accuracy of this method is limited only by the available CPU time. We note, however, that this standard method *assumes* a clean asymptotic power law scaling, which for DP is indeed the case. However, in some cases the power law may be superposed by slowly varying deviations, e.g. logarithmic corrections, so that the plotted data at criticality is actually not straight but slightly curved. With the method outlined above one is then tempted to 'compensate' this curvature by tuning the control parameter, leading to unknown systematic errors. Recently this happened, for example, in the case of the diffusive pair contact process, as will be described in Sect. 3.4.

2.3. The Domany-Kinzel cellular automaton

An important model for DP, which includes directed bond percolation as a special case, is the celebrated Domany-Kinzel model [17,18]. The Domany-Kinzel model is a stochastic cellular automaton defined on a diagonal square lattice which evolves by parallel updates according to certain conditional transition probabilities $P[s_i(t+1)|s_{i-1}(t), s_{i+1}(t)]$, where $s_i(t) \in \{0, 1\}$ denotes the occupancy of site i at time t. These probabilities depend on two parameters p_1, p_2 and are defined by

$$P[1|0, 0] = 0 \ ,$$

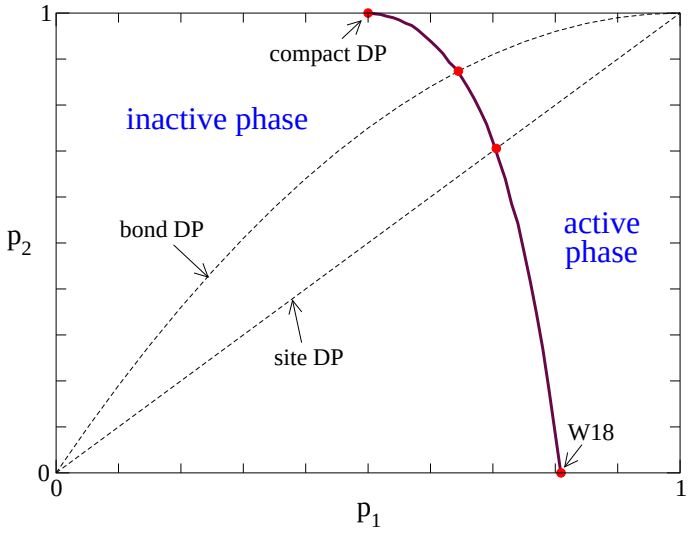

Figure 8. Phase diagram of the Domany-Kinzel model.

$$P[1|0,1] = P[1|1,0] = p_1 \ , \qquad (7)$$
$$P[1|1,1] = p_2 \ ,$$

with $P[0|\cdot,\cdot] = 1 - P[1|\cdot,\cdot]$. On a computer the Domany-Kinzel model can be implemented as follows. To determine the state $s_i(t)$ of site i at time t we generate for each site a random number $z \in (0,1)$ from a flat distribution and set

$$s_i(t+1) = \begin{cases} 1 & \text{if } s_{i-1}(t) \neq s_{i+1}(t) \quad \text{and } z_i(t) < p_1 \ , \\ 1 & \text{if } s_{i-1}(t) = s_{i+1}(t) = 1 \text{ and } z_i(t) < p_2 \ , \\ 0 & \text{otherwise .} \end{cases} \qquad (8)$$

This means that a site is activated with probability p_2 if the two nearest neighbors at the previous time step were both active while it is activated with probability p_1 if only one of them was active. Thus the model depends on *two* percolation probabilities p_1 and p_2, giving rise to the two-dimensional phase diagram shown in Fig. 8. The active and the inactive phase are now separated by a line of phase transitions. This line includes several special cases. For example, the previously discussed case of directed bond percolation corresponds to the choice $p_1 = p$ and $p_2 = p(2-p)$. Another special case is directed site percolation [9], corresponding to the choice $p_1 = p_2 = p$. In this case all bonds are open but sites are permeable with probability p and blocked otherwise. Finally, the special case $p_2 = 0$ is a stochastic generalization of the rule 'W18' of Wolfram's classification scheme of cellular automata [19]. Numerical estimates for the corresponding critical parameters are listed in Table 1.

There is strong numerical evidence that the critical behavior along the whole phase transition line (except for its upper terminal point) is that of DP, meaning that the transitions always exhibit the same type of long-range correlations. The short-range correlations, however, are non-universal and may change when moving along the phase transition line. They may even change the visual appearance of the clusters, as illustrated in Fig. 9, where four typical snapshots of critical clusters are compared.

transition point	$p_{1,c}$	$p_{2,c}$	Ref.
Wolfram rule 18	0.801(2)	0	[20]
site DP	0.70548515(20)	0.70548515(20)	[16]
bond DP	0.644700185(5)	0.873762040(3)	[16]
compact DP	1/2	1	[9]

Table 1. Special transition points in the (1+1)-dimensional Domany-Kinzel model.

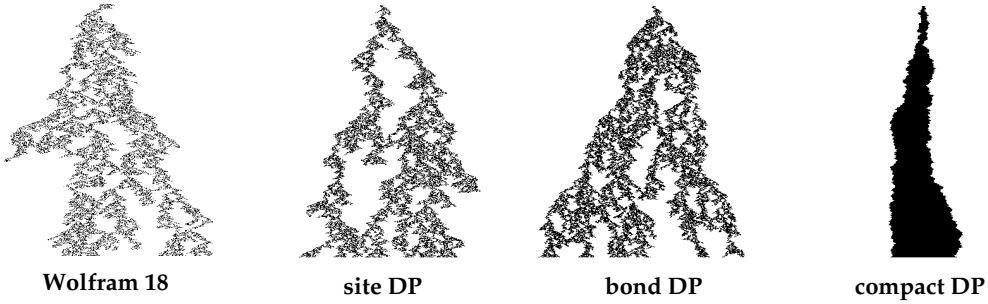

Figure 9. Domany-Kinzel model: Critical cluster generated from a single active seed at different points along the phase transition line (see text).

Although the large-scale structure of the clusters in the first three cases is roughly the same, the microscoppic texture seems to become bolder as we move up along the phase transition line. As shown in Ref. [14], this visual impression can be traced back to an increase of the mean size of active islands.

Approaching the upper terminal point the mean size of active islands diverges and the cluster becomes compact. For this reason this special point is usually referred to as *compact directed percolation*. However, this nomenclature may be misleading for the following reasons. The exceptional behavior at this point of is due to an additional symmetry between active and inactive sites along the upper border of the phase diagram at $p_2 = 1$. Here the DK model has *two* symmetric absorbing states, namely, the empty and the fully occupied lattice. For this reason the transition does no longer belong to the universality class of directed percolation, instead it becomes equivalent to the (1+1)-dimensional voter model [2, 21] or the Glauber-Ising model at zero temperature. Since the dynamic rules are invariant under the replacement $p_1 \leftrightarrow 1 - p_1$, the corresponding transition point is located at $p_1 = 1/2$.

The Domany-Kinzel model can be generalized easily to higher spatial dimensions. For example, Fig. 10 shows a possible cluster in 2+1-dimensional directed bond percolation. Generally, in the d+1-dimensional Domany-Kinzel model the activation probability of site i at time $t + 1$ depends on the number $n_i(t) = \sum_{j \in <i>} s_j(t)$ of active nearest neighbors at time t, i.e. the conditional probabilities

$$\begin{aligned} &P[1|0] = 0 \ , \\ &P[1|n] = p_n \ , \qquad (1 \le n \le 2d) \end{aligned} \tag{9}$$

are controlled by $2d$ parameters $p_1, \ldots, p_{2d}$. The special case of directed bond percolation corresponds to the choice $p_n = 1-(1-p)^n$ while for equal parameters $p_n = p$ one obtains directed site percolation in d+1 dimensions.

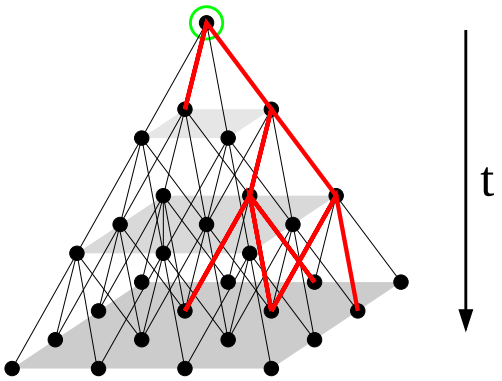

Figure 10. Lattice geometry of directed bond percolation in 2+1 dimensions. The red lines represent a possible cluster generated at the origin.

2.4. The contact process

Another important model for directed percolation, which is popular in mathematical communities, is the contact process. The contact process was originally introduced by Harris [22] as a model for epidemic spreading (see Sect. 4). It is defined on a d-dimensional square lattice whose sites can be either active ($s_i(t) = 1$) or inactive ($s_i(t) = 0$). In contrast to the Domany-Kinzel model, which is a stochastic cellular automaton with parallel updates, the contact process evolves by *asynchronous* updates, i.e., the three elementary processes (offspring production, on-site removal and diffusive moves) occur spontaneously at certain *rates*. Although the microscopic dynamics differs significantly from the Domany-Kinzel model, the contact process displays the same type of critical behavior at the phase transition. In fact, both models belong to the universality class of DP.

On a computer the d+1-dimensional contact process can be implemented as follows. For each attempted update a site i is selected at random. Depending on its state $s_i(t)$ and the number of active neighbors $n_i(t) = \sum_{j\in<i>} s_j(t)$ a new value $s_i(t+dt) = 0, 1$ is assigned according to certain transition rates $w[s_i(t) \to s_i(t+dt), n_i(t)]$. In the standard contact process these rates are defined by

$$w[0 \to 1, n] = \lambda n/2d \ , \tag{10}$$

$$w[1 \to 0, n] = 1 \ . \tag{11}$$

Here the parameter λ plays the same role as the percolation probability in directed bond percolation. Its critical value depends on the dimension d. For example, in 1+1 dimensions the best-known estimate is $\lambda_c \simeq 3.29785(8)$ [23].

As demonstrated in Ref. [14] the evolution of the contact process can be described in terms of a master equation whose Liouville operator $\mathcal{L}$ can be constructed explicitely on a finite lattice. Diagonalizing this operator numerically one obtains a spectrum of relaxational modes with at least one zero mode which represents the absorbing state. In the limit of large lattices the critical threshold λ_c is usually the point from where on the first gap in the spectrum of $\mathcal{L}$ vanishes.

2.5. The critical exponents $\beta, \beta', \nu_\perp$, and $\nu_\parallel$

In equilibrium statistical physics, continuous phase transitions as the one in the Ising model can be described in terms of a phenomenological scaling theory. For example, the spontaneous magnetization M in the ordered phase vanishes as $|M| \sim (T_c - T)^\beta$ as the critical point is approached. Here β is a universal critical exponent, i.e. its value is independent of the specific realization of the model. Similarly, the correlation length ξ diverges in as $\xi \sim |T - T_c|^{-\nu}$ for $T \to T_c$ with another universal exponent ν. The critical point itself is characterized by the absence of a macroscopic length scale so that the system is invariant under suitable scaling transformations (see below).

In directed percolation and other non-equilibrium phase transitions into absorbing states the situation is very similar. However, as non-equilibrium system involves time which is different from space in character, there are now *two* different correlation lengths, namely, a spatial correlation length $\xi_\perp$ and a temporal correlation length $\xi_\parallel$ with two different associated exponents $\nu_\perp$ and $\nu_\parallel$. Their ratio $z = \nu_\parallel/\nu_\perp$ is called *dynamical exponent* as it relates spatial and temporal scales at criticality.

What is the analogon of the magnetization in DP? As shown above, in absorbing phase transitions the choice of the order parameter depends on the initial configuration. If homogeneous initial conditions are used, the appropriate order parameter is the density of active sites at time t

$$\rho(t) = \lim_{L\to\infty} \frac{1}{L} \sum_i s_i(t)\,. \tag{12}$$

Here the density is defined as a spatial average in the limit of large system sizes $L \to \infty$. Alternatively, for a finite system with periodic boundary conditions we may express the density as

$$\rho(t) = \langle s_i(t) \rangle\,, \tag{13}$$

where $\langle \ldots \rangle$ denotes the ensemble average over many realizations of randomness. Because of translational invariance the index i is arbitrary. Finally, if the process starts with a single seed, possible order parameters are the average mass of the cluster

$$N(t) = \langle \sum_i s_i(t) \rangle \tag{14}$$

and the survival probability

$$P(t) = \langle 1 - \prod_i (1 - s_i(t)) \rangle\,. \tag{15}$$

These quantities allow us to define the four standard exponents

$$\rho(\infty) \sim (p - p_c)^\beta\,, \tag{16}$$
$$P(\infty) \sim (p - p_c)^{\beta'}\,, \tag{17}$$
$$\xi_\perp \sim |p - p_c|^{-\nu_\perp}\,, \tag{18}$$
$$\xi_\parallel \sim |p - p_c|^{-\nu_\parallel}\,. \tag{19}$$

The necessity of two different exponents β and β' can be explained in the framework of a field-theoretic treatment, where these exponents are associated with particle creation and annihilation operators, respectively. In DP, however, a special symmetry, called rapidity reversal symmetry, ensures that $\beta = \beta'$. This symmetry can be proven most easily in the case of directed bond percolation, where the density $\rho(t)$ starting from a fully occupied lattice and the survival probability $P(t)$ for clusters grown from a seed are exactly equal for all t. Hence both quantities scale identically and the two corresponding exponents have to be equal. This is the reason why DP is characterized by only three instead of four critical exponents.

The cluster mass $N(t) \sim t^\theta$ scales algebraically as well. The associated exponent, however, is not independent, instead it can be expressed in terms of the so-called *generalized hyperscaling relation* [24]

$$\theta = \frac{d\nu_\perp - \beta - \beta'}{\nu_\parallel} \,. \tag{20}$$

In order to determine the critical point of a given model by numerical methods, $N(t)$ turned out to be one of the most sensitive quantities.

2.6. Scaling laws

Starting point of a phenomenological scaling theory for absorbing phase transitions is the assumption that the macroscopic properties of the system close to the critical point are invariant under scaling transformations of the form

$$\Delta \to a\,\Delta, \quad \mathbf{x} \to a^{-\nu_\perp}\mathbf{x}, \quad t \to a^{-\nu_\parallel} t, \quad \rho \to a^\beta \rho, \quad P \to a^{\beta'} P, \tag{21}$$

where $a > 0$ is some scaling factor and $\Delta = p - p_c$ denotes the distance from criticality. Scaling invariance strongly restricts the form of functions. For example, let us consider the decay of the average density $\rho(t)$ at the critical point starting with a fully occupied lattice. This quantity has to be invariant under rescaling, hence $\rho(t) = a^\beta \rho(t\, a^{-\nu_\parallel})$. Choosing a such that $t\, a^{-\nu_\parallel} = 1$ we arrive at $\rho(t) = t^{-\beta/\nu_\parallel}\rho(1)$, hence

$$\rho(t) \sim t^{-\delta} \,, \qquad \delta = \beta/\nu_\parallel \,. \tag{22}$$

Similarly, starting from an initial seed, the survival probability $P_s(t)$ decays as

$$P_s(t) \sim t^{-\delta'} \,, \qquad \delta' = \beta'/\nu_\parallel \tag{23}$$

with $\delta = \delta'$ in the case of DP.

In an off-critical finite-size system, the density $\rho(t, \Delta, L)$ and the survival probability $P(t, \Delta, L)$ depend on three parameters. By a similar calculation it is easy to show that scaling invariance always reduces the number of parameters by 1, expressing the quantity of interest by a leading power law times a *scaling function* that depends on scaling-invariant arguments. Such expressions are called *scaling forms*. For the density and the survival probability these scaling forms read

$$\rho(t, \Delta, L) \;\sim\; t^{-\beta/\nu_\parallel}\, f(\Delta\, t^{1/\nu_\parallel},\, t^{d/z}/L) \,, \tag{24}$$

$$P(t, \Delta, L) \;\sim\; t^{-\beta'/\nu_\parallel}\, f'(\Delta\, t^{1/\nu_\parallel},\, t^{d/z}/L) \,. \tag{25}$$

critical	MF	$d = 1$	$d = 2$	$d = 3$	$d = 4 - \epsilon$
β	1	0.276486(8)	0.584(4)	0.81(1)	$1 - \epsilon/6 - 0.01128\,\epsilon^2$
$\nu_\perp$	1/2	1.096854(4)	0.734(4)	0.581(5)	$1/2 + \epsilon/16 + 0.02110\,\epsilon^2$
$\nu_\parallel$	1	1.733847(6)	1.295(6)	1.105(5)	$1 + \epsilon/12 + 0.02238\,\epsilon^2$
z	2	1.580745(10)	1.76(3)	1.90(1)	$2 - \epsilon/12 - 0.02921\,\epsilon^2$
δ	1	0.159464(6)	0.451	0.73	$1 - \epsilon/4 - 0.01283\,\epsilon^2$
θ	0	0.313686(8)	0.230	0.12	$\epsilon/12 + 0.03751\,\epsilon^2$

Table 2. Critical exponents of directed percolation obtained by mean field (MF), numerical, and field-theoretical methods.

2.7. Universality

As outlined in the introduction, the working hypothesis in the field of continuous non-equilibrium phase transitions is the notion of *universality*. This concept expresses the expectation that the critical behavior of such transitions can be associated with a finite set of possible universality classes, each corresponding to a certain type of underlying field theory. The field-theoretic action involves certain relevant operators whose form is usually determined by the symmetry properties of the process, while other details of the microscopic dynamics lead to contributions which are irrelevant in the field-theoretic sense. This explains why various different models may belong to the same universality class.

In particular the DP class – the "Ising" class of non-equilibrium statistical physics – is extremely robust with respect to the microscopic dynamic rules. The large variety and robustness of DP models led Janssen and Grassberger to the conjecture that a model should belong to the DP universality class if the following conditions hold [25, 26]:

(i) The model displays a continuous phase transition from a *fluctuating* active phase into a *unique* absorbing state.

(ii) The transition is characterized by a *positive one-component* order parameter.

(iii) The dynamic rules involve only *short-range* processes.

(iv) The system has no unconventional attributes such as additional symmetries or quenched randomness.

Although this conjecture has not yet been proven rigorously, it is highly supported by numerical evidence. In fact, DP seems to be even more general and has been identified even in systems that violate some of the four conditions.

The universality classes can be characterized in terms of their critical exponents and scaling functions. Hence in order to identify a certain universality class, a precise estimation of the critical exponents is an important numerical task. In the case of DP, the numerical estimates suggest that the critical exponents are given by *irrational* numbers rather than simple rational values. In addition, scaling functions (such as f and f' in Eq. (24)), which were ignored in the literature for long time, provide a wealth of useful information, as shown e.g. in a recent review by Lübeck [13].

2.8. Langevin equation

On a coarse-grained level DP is often described in terms of a phenomenological Langevin equation with a field-dependent noise. This Langevin equation can be derived rigorously from the master equation of the contact process [25] and reads

$$\partial_t \rho(\mathbf{x},t) \;=\; a\rho(\mathbf{x},t) - \lambda\rho^2(\mathbf{x},t) + D\nabla^2\rho(\mathbf{x},t) + \xi(\mathbf{x},t)\;. \tag{26}$$

Here $\xi(\mathbf{x},t)$ is a density-dependent Gaussian noise field with the correlations

$$\langle \xi(\mathbf{x},t)\rangle \qquad\quad = 0\,, \tag{27}$$

$$\langle \xi(\mathbf{x},t)\xi(\mathbf{x}',t')\rangle = \Gamma\,\rho(\mathbf{x},t)\,\delta^d(\mathbf{x}-\mathbf{x}')\,\delta(t-t')\;. \tag{28}$$

Since the amplitude of $\xi(\mathbf{x},t)$ is proportional to $\sqrt{\rho(\mathbf{x},t)}$, the absorbing state $\rho(\mathbf{x},t)=0$ does not fluctuate. The square-root behavior is related to the fact that the noise describes density fluctuations on a coarse-grained scale, which can be viewed as the sum of individual noise contributions generated by each particle averaged over some mesoscopic box size. According to the central limit theorem, if the number of particles in this box is sufficiently high, $\xi(\mathbf{x},t)$ approaches a Gaussian distribution with an amplitude proportional to the square root of the number of active sites in the box.

Applying the scaling transformation (21) to Eqs. (26)-(27) a simple dimensional analysis gives the mean field critical point $a_c = 0$ and the mean field exponents

$$\beta^{\rm MF} = \beta'^{\rm MF} = 1, \quad \nu_\perp^{\rm MF} = 1/2, \quad \nu_\parallel^{\rm MF} = 1. \tag{29}$$

In this situation the noise is irrelevant in $d > 4$, marginal in $d = 4$, and relevant in $d < 4$ dimensions. This means that $d_c = 4$ is the *upper critical dimension* of directed percolation above which the mean field exponents are correct. Below d_c the exponents can be determined by a renormalization group study of the corresponding field theory. A comprehensive introduction to the field theory of DP and other universality classes is beyond the scope of these lecture notes, the interested reader is referred to very recent and excellent review articles by Janssen, Täuber, Howard, and Lee [27, 28]. We note that Eq. (26) is the minimal Langevin equation needed to describe DP. It may also include higher order terms such as $\rho^3(\mathbf{x},t)$, $\nabla^4\rho(\mathbf{x},t)$, or higher-order contributions of the noise, but in the field-theoretic sense these contributions turn out to be irrelevant under renormalization group transformations, explaining the robustness of DP.

2.9. Multifractal properties of currents on directed percolation clusters

So far we have seen that the critical behavior of DP and other absorbing phase transitions can be described in terms of scaling laws that involve three independent critical exponents β, $\nu_\perp$, and $\nu_\parallel$. This type of scaling is usually referred to as *simple scaling*, as opposed to multiscaling, where a whole spectrum of exponents exists. For example, in DP at criticality starting with a homogeneous initial state any integral power ρ^n of the order parameter ρ scales in the same way, i.e.

$$\rho^n(t) \sim t^{-\delta} \qquad n = 1, 2, 3, \ldots\,. \tag{30}$$

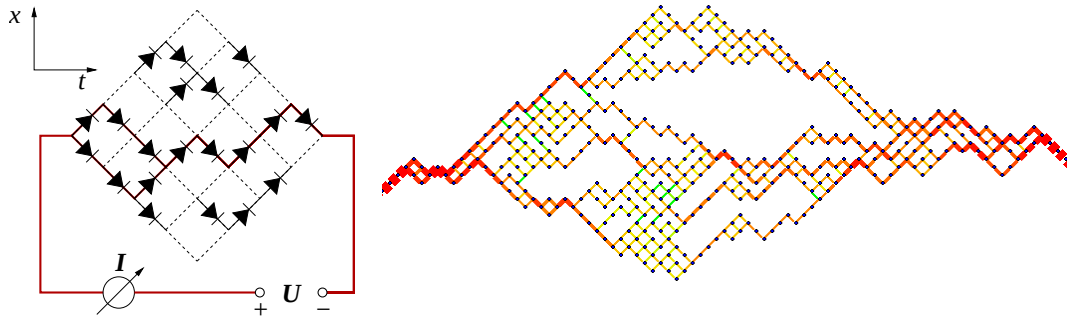

Figure 11. Electric current running through a random resistor-diode network at the percolation threshold from one point to the other. The right panel shows a particular realization. The color and thickness of the line represent the intensity of the current.

Let us now consider an electric current running on a directed percolation cluster according to Kirchhoff's laws, interpreting the cluster as a random resistor-diode network. By introducing such a current the theory is extended by an additional physical concept. In fact, even though the DP cluster itself is known to be characterized by simple scaling laws, a current running on it turns out to be distributed in a *multifractal* manner. This phenomenon was first discovered in the case of isotropic percolation [29, 30] and then confirmed for DP [31, 32].

As shown in Fig. 11, in directed bond percolation at criticality an electric current I running from one point to the other is characterized by a non-trivial distribution of currents. The multifractal structure of this current distribution can be probed by studying the moments

$$M_\ell := \sum_b (I_b/I)^\ell \qquad \ell = 0, 1, 2, \dots \,, \tag{31}$$

where the sum runs over all bonds b that transport a non-vanishing current $I_b > 0$. For example, M_0 is just the number of conducting bonds while M_1 is essentially the total resistance between the two points. M_2 is the second cumulant of the resistance fluctuations and can be considered as a measure of the noise in a given realization. Finally, M_∞ is the number of so-called red bonds that carry the full current I. The quantity M_ℓ is found to scale as a power law

$$M_\ell(t) \sim t^{\psi_\ell/\nu_\parallel} \,. \tag{32}$$

In the case of simple scaling, the exponents ψ_ℓ would depend linearly on ℓ. In the present case, however, a non-linear dependence is found both by field-theoretic as well as numerical methods (see Ref. [32]). This proves that electric currents running on DP clusters have multifractal properties.

Again it should be emphasized that multifractality is not a property of DP itself, rather it emerges as a new feature whenever an additional process, here the transport of electric currents, is confined to live on the critical clusters of DP.

2.10. Characterizing non-equilibrium transition by Yang-Lee zeroes in the complex plane

In equilibrium statistical mechanics a large variety of continuous phase transitions has been analyzed by studying the distribution of so-called Yang-Lee zeros [33–35]. To determine these zeros the partition sum of a (finite) equilibrium system is expressed as a polynomial of the control parameter, which is usually a function of temperature. E.g., for the Ising model the zeros of this polynomial lie on a circle in the complex plane and heckle the real line from both sides in the vicinity of the phase transition as the system size increases. This explains why the analytic behavior in finite system crosses over to a non-analytic behavior at the transition point in the thermodynamic limit.

Recently, it has been shown that the concept of Yang and Lee can also be applied to non-equilibrium systems [36], including DP [37]. To this end one has to consider the order parameter in a finite percolation tree as a function of the percolation probability p in the complex plane. This can be done by studying the survival probability $P(t)$ (see Eq. (15)), which is defined as the probability that a cluster generated in a single site at time $t = 0$ survives at least up to time t. In fact, the partition sum of an equilibrium system and the survival probability of DP are similar in many respects. They both are positive in the physically accessible regime and can be expressed as polynomials in finite systems. As the system size tends to infinity, both functions exhibit a non-analytic behavior at the phase transition as the Yang-Lee zeros in the complex plane approach the real line.

In directed bond percolation the survival probability is given by the sum over the weights of all possible configurations of bonds, where each conducting bond contributes to the weight with a factor p, while each non-conducting bond contributes with a factor $1-p$. As shown in Ref [37], the polynomial for the survival probability can be expressed as a sum over all cluster configurations c reaching the horizontal row at time t. The polynomial is of the form

$$P(t) = \sum_c p^n (1-p)^m \,, \tag{33}$$

where n denotes the number of bonds while m is the number of bonds belonging to its cluster's hull. Summing up all weights in Eq. (33), one obtains a polynomial of degree $t^2 + t$. For example, the first few polynomials are given by

$$\begin{aligned}
P(0) &= 1 \\
P(1) &= 2p - p^2 \\
P(2) &= 4p^2 - 2p^3 - 4p^4 + 4p^5 - p^6 \\
P(3) &= 8p^3 - 4p^4 - 10p^5 - 3p^6 + 18p^7 + 5p^8 - 30p^9 + 24p^{10} - 8p^{11} + p^{12} \\
P(4) &= 16p^4 - 8p^5 - 24p^6 - 8p^7 + 6p^8 + 84p^9 - 29p^{10} - 62p^{11} - 120p^{12} \\
&\quad + 244p^{13} + 75p^{14} - 470p^{15} + 495p^{16} - 268p^{17} + 83p^{18} - 14p^{19} + p^{20}
\end{aligned} \tag{34}$$

As t increases, the number of cluster configurations grows rapidly, leading to complicated polynomials with very large coefficients. The distribution of zeros in the complex plane for $t = 15$ is shown in Fig. 12. As can be seen, the distribution reminds of a fractal, perhaps being a signature of the non-integrable nature of DP. As expected, the

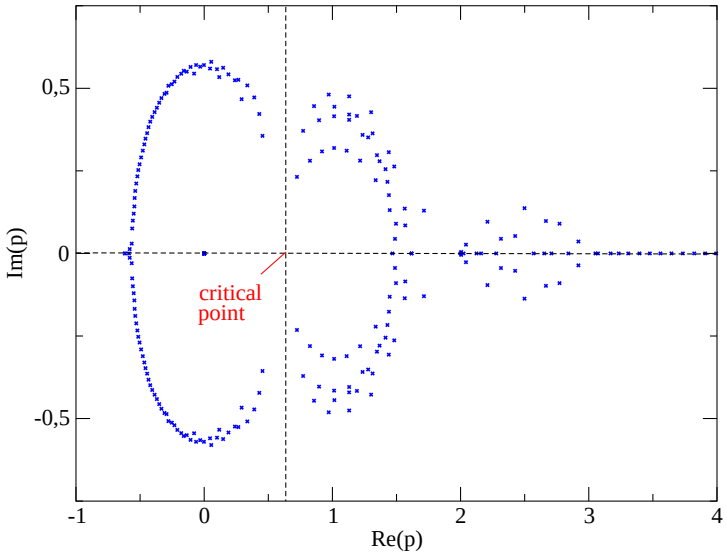

Figure 12. Distribution of Yang-Lee zeros of the polynomial $P(15)$ in the complex plane. The transition point is marked by an arrow.

zeros approach the phase transition point from above and below. Their distance to the transition point is found to scale as $t^{-1/\nu_\parallel}$ in agreement with basic scaling arguments.

3. Other classes of absorbing phase transitions

So far we discussed directed percolation as the most important class of non-equilibrium phase transitions into absorbing states. Because of the robustness of DP it is interesting to search for other universality classes. The ultimate goal would be to set up a table of possible non-trivial universality classes from active phases into absorbing states.

Although various exceptions from DP have been identified, the number of firmly established universality classes is still small. A recent summary of the *status quo* can be found in Refs. [12, 13]. In these lecture notes, however, we will only address the most important classes with local interactions.

3.1. Parity-conserving particle processes

The parity-conserving (PC) universality class comprises phase transitions that occur in reaction-diffusion processes of the form

$$A \to (n+1)A \tag{35}$$
$$2A \to \emptyset \tag{36}$$

combined with single-particle diffusion, where the number of offspring n is assumed to be even. As an essential feature, these processes conserve the number of particles modulo 2. A particularly simple model in this class with $n = 2$ was proposed by Zhong

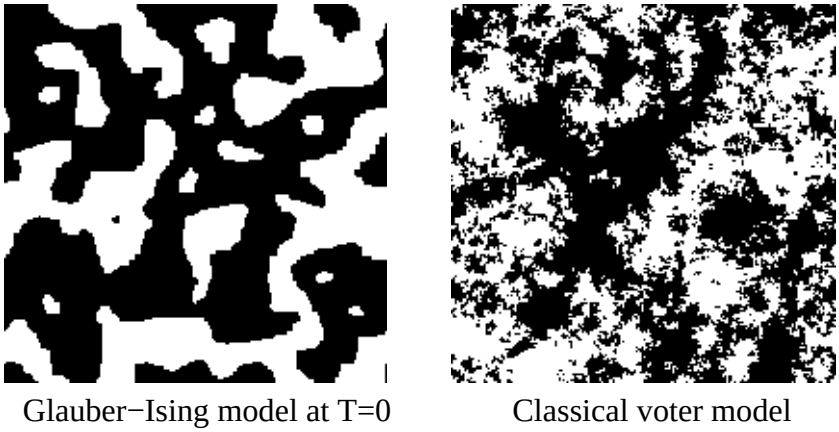

Figure 13. Coarsening of a random initial state in the Glauber-Ising model at zero temperature compared to the coarsening in the classical voter model.

and ben-Avraham [38]. The estimated critical exponents

$$\beta = \beta' = 0.92(2)\,, \quad \nu_\parallel = 3.22(6)\,, \quad \nu_\perp = 1.83(3) \tag{37}$$

differ significantly from those of DP, establishing PC transitions as an independent universality class. The actual values of δ and θ depend on the initial condition. If the process starts with a single particle, it will never stop because of parity conservation, hence $\delta = 0$, i.e. the usual relation $\delta = \beta/\nu_\parallel$ does no longer hold. However, if it starts with two particles, the roles of δ and θ are exchanged, i.e. $\theta = 0$. The theoretical reasons for this exchange are not yet fully understood.

The relaxational properties in the subcritical phase differ significantly from the standard DP behavior. While the particle density in DP models decays exponentially as $\rho(t) \sim e^{-t/\xi_\parallel}$, in PC models it decays algebraically since the decay is governed by the annihilation process $2A \to \emptyset$.

A systematic field theory for PC models can be found in Refs. [39, 40], confirming the existence of the annihilation fixed point in the inactive phase. However, the field-theoretic treatment at criticality is extremely difficult as there are *two* critical dimensions: $d_c = 2$, above which mean-field theory applies, and $d_c' \approx 4/3$, where for $d > d_c'$ ($d < d_c'$) the branching process is relevant (irrelevant) at the annihilation fixed point. Therefore, the physically interesting spatial dimension $d = 1$ cannot be accessed by a controlled ϵ-expansion down from upper critical dimension $d_c = 2$.

3.2. The voter universality class

Order-disorder transition in models with a Z_2-symmetry which are driven by *interfacial noise* belong to the so-called voter universality class [21]. As will be explained below, the voter class and the parity conserving class are identical in one spatial dimension but different in higher dimensions.

To understand the physical mechanism that generates the phase transition in the voter model, let us first discuss the difference between interfacial and bulk noise.

Consider for example the Glauber-Ising model in two spatial dimensions at $T = 0$. This model has two Z_2-symmetric absorbing states, namely, the two fully ordered states. Starting with a random initial configuration one observes a coarsening process forming odered domains whose size grows as $\sqrt{t}$. In the Ising model at $T = 0$ domain growth is curvature-driven, leading to an effective surface tension of the domain walls. In fact, as shown in Fig. 13 the domain walls produced by the Glauber-Ising model appear to be smooth and indeed the density of domain walls is found to decay as $1/\sqrt{t}$. Increasing temperature occasional spin flips occur, leading to the formation of small minority islands *inside* the existing domains. For small temperature the influence of surface tension is strong enough to eliminate these minority islands, stabilizing the ordered phase. However, increasing T above a certain critical threshold T_c this mechanism breaks down, leading to the well-known order-disorder phase transition in the Ising model. Thus, from the perspective of a dynamical process, the Ising transition results from a competition between surface tension of domain walls and bulk noise.

Let us now compare the Glauber-Ising model with the classical voter model in two spatial dimensions. The classical voter model [2] is a caricatural process in which sites (voters) on a square lattice adopt the opinion of a randomly-chosen neighbor. As the Ising model, the voter model has two symmetric absorbing states. Moreover, an initially disordered state coarsens. However, as shown in the right panel of Fig. 13, already the visual appearance is very different. In fact, in the voter model the domain sizes are found to be distributed over the whole range between 1 and $\sqrt{t}$. Moreover, in contrast to the Glauber-Ising model, the density of domain walls decays only logarithmically as $1/\ln t$. This marginality of the voter model is usually attributed to the exceptional character of its analytic properties [41–43] and may be interpreted physically as the *absence* of surface tension.

In the voter model even very small thermal bulk noise would immediately lead to a disordered state. However, adding *interfacial noise* one observes a non-trivial continuous phase transition at a finite value of the noise amplitude. Unlike bulk noise, which flips spins everywhere inside the ordered domains, interfacial noise restricts spin flips to sites in the vicinity of domain walls.

Recently Al Hammal *et al* [44] introduced a Langevin equation describing voter transitions. It is given by

$$\frac{\partial}{\partial t}\rho = (a\rho - b\rho^3)(1-\rho^2) + D\nabla^2\rho + \sigma\sqrt{1-\rho^2}\,\xi\,, \tag{38}$$

where ξ is a Gaussian noise with constant amplitude. For $b > 0$ this equation is found to exhibit separate Ising and DP transitions, while for $b \leq 0$ a genuine voter transition is observed. With these new results the voter universality class is now on a much firmer basis than before.

In one spatial dimension, kinks between domain walls can be interpreted as particles. Here interfacial noise between two domains amounts to generating pairs of additional domain walls nearby. This process, by its very definition, conserves parity and can be interpreted as offspring production $A \to 3A, 5A, \ldots$ while pairwise coalescence of domain walls corresponds to particle annihilation $2A \to \emptyset$. For this reason the voter class and the parity-conserving class coincide in one spatial dimension. However,

their behavior in higher dimensions, in particular the corresponding field theories, are expected to be different. Loosely speaking, the parity-conserving class deals with the dynamics of zero-dimensional objects (particles), while in the voter class the objects of interest are d-1-dimensional hypermanifolds (domain walls).

3.3. Absorbing phase transitions with a conserved field

According to the conjecture by Janssen and Grassberger (cf. Sect. 2.7), non-DP behavior is expected if the dynamics is constrained by additional conservation laws. For example, as shown in the previous subsections, parity conservation or a Z_2-symmetry may lead to different universality classes. Let us now consider phase transitions in particle processes in which the total number of particles is conserved. According to an idea by Rossi *et al* [45] this leads to a different universality class of phase transitions which is characterized by an effective coupling of the process to a non-diffusive conserved field. Models in this class have infinitely many absorbing states and are related to certain models of self-organized criticality (for a recent review see Ref. [13]).

As an example let us consider the conserved threshold transfer process (CTTP). In this model each lattice site can be vacant or occupied by either one or two particles. Empty and single occupied sites are considered as inactive while double occupied sites are regarded as active. According to the dynamical rules each active site attempts to move the two particles randomly to neighboring sites, provided that these target sites are inactive. By definition of these rules, the total number of particles is conserved. Clearly, it is the background of solitary particles that serves as a conserved field to which the dynamics of active sites is coupled.

In $d \geq 2$ spatial dimensions this model shows the same critical behavior as the Manna sand pile model [46]. The corresponding critical exponents in $d = 2$ dimensions were estimated by [13]

$$\beta = 0.639(9)\,, \quad \beta' = 0.624(29)\,, \quad \nu_\perp = 0.799(14)\,, \quad \nu_\parallel = 1.225(29). \tag{39}$$

Obviously, this set of exponents differs from those of all other classes discussed above. In one spatial dimension the situation is more complicated because of a split of the CTTP and Manna universality classes, as described in detail in Ref. [13]

3.4. The diffusive pair contact process

Among the known transitions into absorbing states, the transition occurring in the so-called contact process with diffusion (PCPD) is probably the most puzzling one (see Ref. [47] for a recent review). The PCPD is a reaction-diffusion process of particles which react spontaneously whenever *two of them* come into contact. In its simplest version the PCPD involves two competing reactions, namely

$$\begin{aligned} &\text{fission:} && 2A \to 3A\,, \\ &\text{annihilation:} && 2A \to \emptyset\,. \end{aligned}$$

In addition individual particles are allowed to diffuse. Moreover, there is an additional mechanism such that the particle density cannot diverge. In models with at most one

particle per site this mechanism is incorporated automatically.

The PCPD displays a non-equilibrium phase transition caused by the competition of fission and annihilation. In the active phase, the fission process dominates, maintaining a fluctuating steady-state, while in the subcritical phase the annihilation process dominates so that the density of particles decreases continuously until the system reaches one of the absorbing states. The PCPD has actually two absorbing states, namely, the empty lattice and a homogeneous state with a single diffusing particle.

The pair-contact process *with* diffusion was already suggested in 1982 by Grassberger [48], who expected a critical behavior "distinctly different" from DP. Eight years ago the problem was rediscovered by Howard and Täuber [49], who proposed a bosonic field-theory for the one-dimensional PCPD. In this theory the particle density is unrestricted and thus diverges in the active phase. The first quantitative study of a restricted PCPD by Carlon *et al* [50] using DMRG techniques led to controversial results and released a still ongoing debate concerning the asymptotic critical behavior of the 1+1-dimensional PCPD at the transition. Currently the main viewpoints are that the PCPD

- represents a new universality class with well-defined critical exponents [51],
- represents *two different* universality classes depending on the diffusion rate [52, 53] and/or the number of space dimensions [54],
- can be interpreted as a cyclically coupled DP and annihilation process [55],
- is a marginally perturbed DP process with continuously varying exponents [56],
- may have exponents depending continuously on the diffusion constant [57],
- may cross over to DP after very long time [58, 59], and
- is perhaps related to the problem of non-equilibrium wetting in 1+1 dimensions [60].

Personally I am in favor of the conjecture that the PCPD in 1+1 dimensions belongs to the DP class. This DP behavior, however, is masked by extremely slow (probably logarithmic) corrections. Searching the critical point by fitting straight lines in a double logarithmic plot may therefore lead to systematic errors in the estimate of the critical threshold since the true critical line is not straight but slightly curved. This in turn leads to even larger systematic errors for the critical exponents. However, as the computational effort is increased, these estimates seem to drift towards DP exponents.

The problem of systematic errors and drifting exponents can be observed for example in the work by Kockelkoren and Chaté, who tried to establish the PCPD as a new universality class as part of a general classification scheme [51]. Introducing a particularly efficient model they observed clean power laws in the decay of the density over several decades, leading to the estimates

$$\delta = \beta/\nu_\parallel = 0.200(5), \quad z = \nu_\perp/\nu_\parallel = 1.70(5), \quad \beta = 0.37(2). \tag{40}$$

However, increasing the numerical effort by a decade in time, it turns out that their critical point $p_c = 0.795410(5)$, including its error margin, lies entirely in the inactive phase (see Fig. 14). In the attempt to obtain an apparent power-law behavior, it seems that the authors systematically underestimated the critical point.

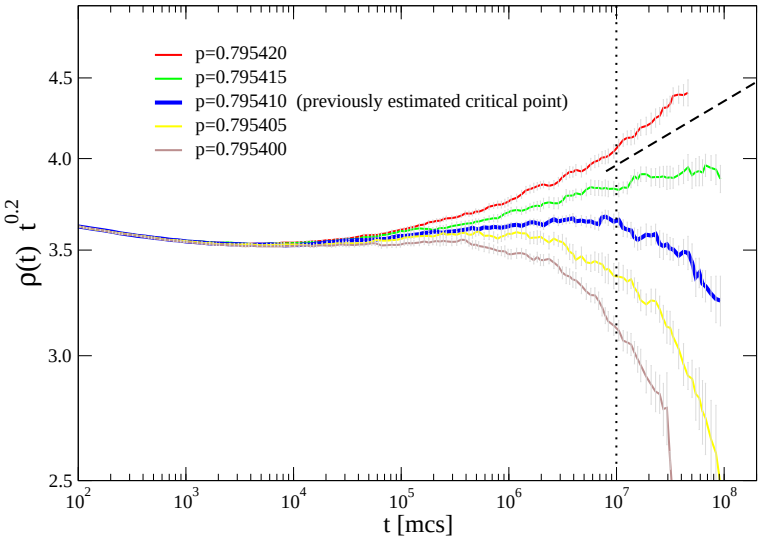

Figure 14. High-performance simulation of the PCPD model introduced by Kockelkoren and Chaté. The plot shows the density of active sites multiplied by the expected power law. As can be seen, the lines are slightly curved. Kockelkoren and Chaté simulated the process up to about 10^7 Monte Carlo updates (dotted line), identifying the blue line in the middle as critical curve. Extending these simulations by one decade one recognizes that this curve is actually subcritical and that the true critical threshold has to be slightly higher. Obviously a slow drift towards DP (slope indicated by dashed line) cannot be excluded.

Presently it is still not yet clear whether the PCPD belongs to the DP universality class or not. Apparently computational methods have reached their limit and more sophisticated techniques are needed to settle this question.

4. Epidemic spreading with long-range interactions

Directed percolation is often used as a caricatural process for epidemic spreading. Suppose that infected and healthy individuals are sitting in a train, as shown in Fig. 15. On the one hand, infected people infect their nearest neighbors with a certain probability per unit time. On the other hand, infected individuals may recover spontaneously. Depending on the rates for infection and recovery, this toy model for epidemic spreading just resembles a simple DP process.

Although DP is too simplistic to describe epidemic spreading in reality, there are some important analogies. Certainly, epidemic spreading in Nature is a non-equilibrium process with a transition-like behavior at some threshold of the infection rate. For example, as an increasing number of people refuses vaccinations, the question arises at which percentage of unprotected individuals certain diseases, that became almost extinct, will again percolate through the society.

Epidemic spreading in Nature is of course a much more complex phenomenon. For example, it takes place in a very disordered environment and involves short- and long-range interactions. Moreover, individuals protect themselves by sophisticated

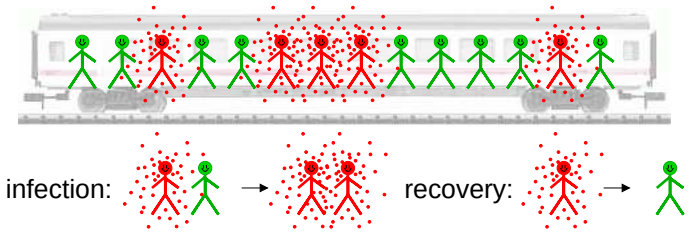

Figure 15. Directed percolation as a caricature of an epidemic process

immunization strategies. Certainly, physicist will never be able to predict epidemic spreading in Nature quantitatively. However, it is possible to extend DP towards a more realistic description of epidemic spreading and to study how they influence the behavior at the transition. Some of these extensions will be discussed in the following.

4.1. Immunization and mutations

As a first step towards a more realistic description of epidemic spreading we may include the effect of immunization. For example, we may declare all sites that were active at least once in the past as immune. One then introduces two different infection probabilities, namely, a probability for first infection p_0, and a second (usually smaller) probability p for the reinfection of immune sites. The case of perfect immunization (vanishing reinfection probability) is known as *general epidemic process* [61] which can be regarded as a dynamical procedure to grow isotropic percolation clusters.

Introducing a finite reinfection probability one obtains the phase diagram shown in Fig. 16. It comprises a curved phase transition line with the same critical behavior as in the generalized epidemic process which separates phases of finite and annular growth. Moreover, there is a horizontal transition line above which compact cluster growth is observed. The critical properties along this line are partly dictated by the DP behavior inside immune regions, combined with non-universal properties for the growth of the clusters at its boundaries [62]. Both transition lines meet in a point with an interesting multicritical behavior. Extending this model by possible mutations of the spreading agent, the memory of immunization is lost. As a result one observes a controlled crossover back to DP [63].

4.2. Long-range infections

Realistic diseases spread by different transport mechanisms, including direct contact between local individuals, transport by carriers such as mosquitos, and long-range transport e.g. by air planes. Usually it is very difficult to predict how these transport mechanism contribute to epidemic spreading. As an interesting empirical approach, Brockmann and Geisel traced the spatio-temporal trajectories of individual dollar notes within the United States [64, 65]. In agreement with previous conjectures [66] they found out that the transport distances are distributed algebraically with some empirical exponent. Moreover, the time intervals at which the dollar notes were registered were found to obey a power law as well.

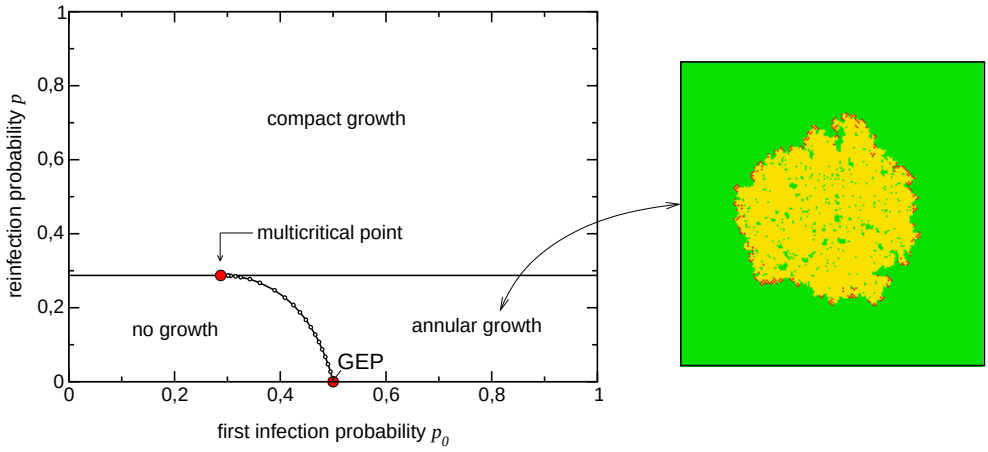

Figure 16. Phase diagram for directed percolation with immunization (see text). The right panel shows spreading by annular growth with fresh (green), active (red), and immune (yellow) individuals.

Motivated by such empirical studies it is near at hand to generalize DP such that the spreading distances r are distributed as a power law

$$P(r) \sim r^{-d-\sigma}\,, \qquad (\sigma > 0) \tag{41}$$

where σ is a control exponent. In the literature such algebraically distributed long-range displacements are known as *Lévy flights* [67] and have been studied extensively e.g. in the context of anomalous diffusion [68]. In the present context of epidemic spreading it turns out that such long-range flights do not destroy the transition, instead they change the critical behavior provided that σ is sufficiently small. More specifically, it was observed both numerically and in mean field approximations that the critical exponents change *continuously* with σ [69–71]. As a major breakthrough, Janssen *et al* introduced a renormalizable field theory for epidemic spreading transitions with spatial Lévy flights [72], computing the critical exponents to one-loop order. Because of an additional scaling relation only two of the three exponents were found to be independent. These results were confirmed numerically by Monte Carlo simulations [73].

4.3. Incubation times

As a second generalization one can introduce a similar long-range mechanism in *temporal* direction. Such 'temporal' Lévy flights may be interpreted as incubation times Δt between catching and passing on the infection. As in the first case, these incubation times are assumed to be algebraically distributed as

$$P(\Delta t) \sim \Delta t^{-1-\kappa}\,, \qquad (\kappa > 0) \tag{42}$$

where κ is a control exponent. However, unlike spatial Lévy flights, which take place equally distributed in all directions, such temporal Lévy flights have to be directed forward in time. Again it was possible to compute the exponents by a field-theoretic renormalization group calculation [74].

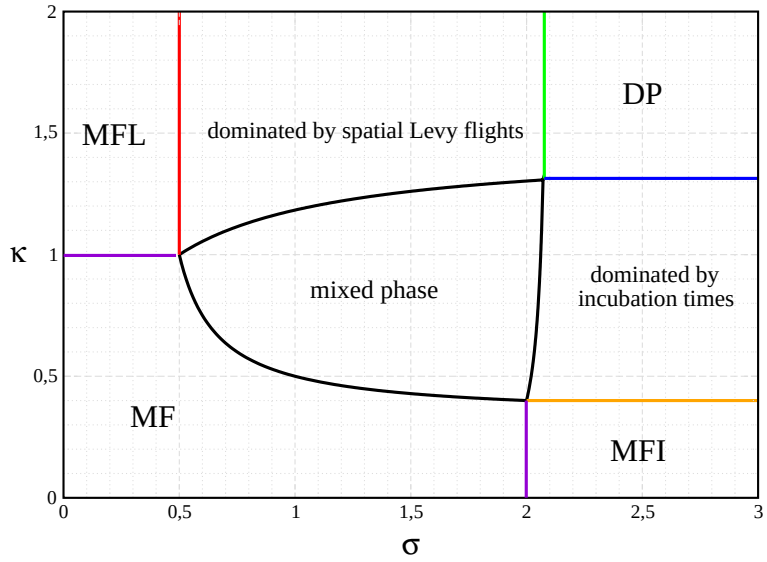

Figure 17. Phase diagram of DP with spatio-temporal Lévy flights.

Recently, we studied the mixed case of epidemic spreading by spatial Lévy flights *combined* with algebraically distributed incubation times [75]. In this case the corresponding field theory was found to render two additional scaling relations, namely,

$$2\beta + (\sigma - d)\nu_\perp - \nu_\parallel = 0\,, \tag{43}$$

$$2\beta - d\nu_\perp + (\kappa - 1)\nu_\parallel = 0\,. \tag{44}$$

Hence only one of the three exponents is independent. In particular, the dynamical exponent z locks onto the ratio σ/κ. A systematic numerical and field-theoretic study leads to a generic phase diagram in terms of the control exponents σ and κ which is shown in Fig. 17. It includes three types of mean-field phases, a DP phase, two phases corresponding to purely spatial or purely temporal Lévy flights, and a novel fluctuation-dominated phase describing the mixed case in which the critical exponents have been computed by a field-theoretic renormalization group calculation to one-loop order.

5. Surface growth and non-equilibrium wetting

Another interesting direction of non-equilibrium physics is the study of *wetting* far from equilibrium. Wetting phenomena occur in a large variety of experiments, where a planar substrate is exposed to a gas phase. Usually the term 'wetting' refers to a situation where a bulk phase in contact with a substrate coexists with a layer of a different phase which is preferentially attracted to the surface of the substrate. By changing physical parameters such as temperature and chemical potential, the system may undergo a wetting transition from a non-wet phase, where the thickness of the layer stays finite, to a wet phase, where the layer becomes macroscopic.

In many experimental situations it is reasonable to assume that a wetting stationary layer is in thermal equilibrium. In fact, methods of equilibrium statistical mechanics turned out to be very successful in a large variety of theoretical and experimental studies [76]. Therefore, the question arises whether models for wetting far from

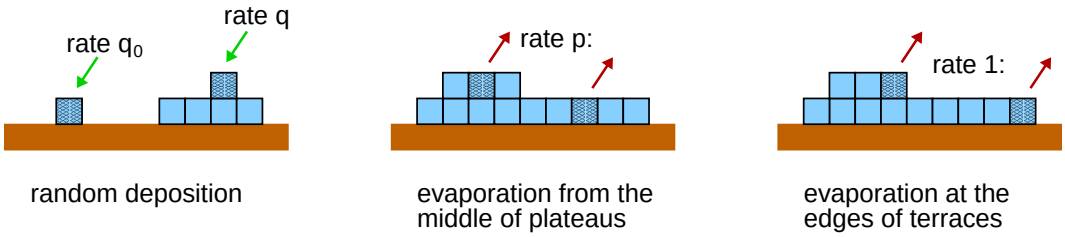

Figure 18. Dynamical rules of the restricted solid-on-solid model for non-equilibrium wetting. Neighboring heights are restricted to differ by at most one unit.

equilibrium may exhibit new physical phenomena which cannot be observed under equilibrium conditions.

Non-equilibrium wetting is usually modeled as a Kardar-Parisi-Zhang (KPZ) growth process [77] growing on top of a hard substrate. Theoretically such a system can be described by a KPZ equation in a potential [78, 79]

$$\frac{\partial h(\mathbf{x},t)}{\partial t} = \sigma\nabla^2 h(\mathbf{x},t) - \frac{\partial V(h(\mathbf{x},t))}{\partial h(\mathbf{x},t)} + \lambda(\nabla h(\mathbf{x},t))^2 + \xi(\mathbf{x},t)\,, \tag{45}$$

where $\xi(\mathbf{x},t)$ is a Gaussian noise. It is important to note that the nonlinear term $\lambda(\nabla h(\mathbf{x},t))^2$ in this equation is a *relevant* perturbation of the underlying field theory, i.e., even if λ is very small, it will be amplified under renormalization group transformations, driving the system away from thermal equilibrium. In fact, as can be shown by constructing a closed loop, it is this term that breaks detailed balance.

Some time ago we introduced a simple solid-on-solid (SOS) model for non-equilibrium wetting in 1+1 dimensions [80–82]. The model is controlled by an adsorption rate q, a desorption rate p, and optionally by a special deposition rate q_0 on sites at height zero (desorption at the edges takes place at rate 1, see Fig. 18). Setting $q_0 = q$ and varying the growth rate the model exhibits a continuous wetting transition at a certain critical growth rate $q_c(p)$. This wetting transition is related to the unpinning process of an interface from the substrate. Moreover, for $q_0 \neq q$ the model can emulate a short-range interaction between the interface and the substrate [83,84]. It was found that sufficiently strong attractive interaction modifies the nature of the wetting transition and makes it first order. In addition, it has been demonstrated that there exists an extended region in the phase diagram, where the pinned and the moving phases *coexist* in the sense that the transition time from the pinned to the moving phase grows exponentially with the system size so that the two phases become stable in the thermodynamic limit. This type of phase coexistence is in fact a new phenomenon that occurs only far away from equilibrium and should be experimentally observable.

6. Summary

At the end of this lecture let us address the crucial question to what extent these recent developments in the field of non-equilibrium statistical physics can be confirmed experimentally. Unfortunately, the experimental evidence is still very poor. For example, although many transition-like phenomena far from equilibrium can be seen

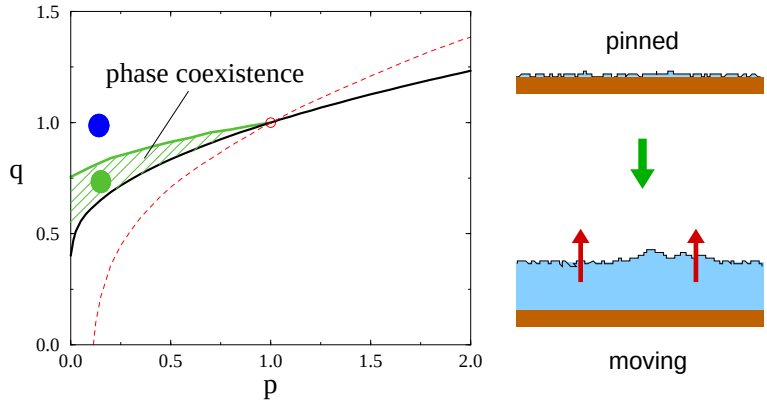

Figure 19. Phase diagram of the solid-on-solid model for non-equilibrium wetting. The bold black line represents the second-order phase transition line. For sufficiently small q_0 the transition becomes first order and a region emerges (striped in the figure), where the pinned and the moving phase coexist.

in Nature, there is so far *no* experiment in which the exponents of DP or any other class of absorbing phase transitions can be reproduced quantitatively in a reliable way. This is surprising since various possible experimental realizations have been proposed [85]. For deposition-evaporation phenomena the situation is not much better: Up to now no convincing experiment is known in which the exponents of the KPZ universality class can be confirmed.

The poor experimental evidence could be partly due to the fact that many experimentalists are not yet fully aware of recent developments in non-equilibrium statistical physics. Similarly, many theoretical physicists do not care so much about experiments and regard instead the computer as the beauty of Nature. However, the poor experimental evidence could have more fundamental reasons. For example, despite the robustness and simplicity of DP, the existence of an absorbing state is a highly idealized requirement that is difficult to realize experimentally.

With the advent of modern nanotechnology, however, the situation could change in near future. Therefore, it is particularly important to understand the crossover between quantum and classical behavior in order to find out where the models of non-equilibrium statistical physics can be applied. All in all we should be optimistic: Universality classes which are as fundamental as DP or KPZ are so beautiful that they should be relevant in Nature. In fact, in equilibrium statistical mechanics there was quite a long way from Onsagers solution of the two-dimensional Ising model to the ample experimental evidence that is available today.

References

[1] E. Joos, H. D. Zeh, C. Kiefer, D. Giulini, J. Kupsch, and I.-O. Stamatescu, *Decoherence and the appearance of a classical world in quantum theory*, Springer, Berlin, 2003.

[2] T. M. Liggett, *Interacting particle systems*, Springer, Berlin, 1985.

[3] H. Spohn, *Large scale dynamics of interacting particles*, Springer, Berlin, 1991.

[4] A. M. Polyakov, Conformal symmetry of critical fluctuations, Sov. Phys. JETP Lett. **12**, 381 (1970).

[5] J. L. Cardy, Conformal Invariance, in *Phase transitions and critical phenomena*, edited by

C. Domb and J. L. Lebowitz, volume 11, Academic Press, New York, 1987.
[6] M. Henkel, *Conformal Invariance and Critical Phenomena*, Springer Verlag, Berlin, 1999.
[7] A. L. Barabási and H. Stanley, *Fractal concepts in surface growth*, Cambridge University Press, U.K., 1995.
[8] D. E. Wolf, M. Schreckenberg, and A. Bachem, *Traffic and granular flow*, World Scientific, Singapore, 1996.
[9] W. Kinzel, Percolation structures and processes, in *Ann. Isr. Phys. Soc.*, edited by G. Deutscher, R. Zallen, and J. Adler, volume 5, Adam Hilger, Bristol, 1983.
[10] J. Marro and R. Dickman, *Nonequilibrium phase transitions in lattice models*, Cambridge University Press, Cambridge, 1999.
[11] P. Grassberger, Directed percolation: results and open problems, in *Nonlinearities in complex systems, proceedings of the 1995 Shimla conference on complex systems*, edited by S. Puri *et al.*, Narosa Publishing, New Dehli, 1997.
[12] G. Ódor, Universality classes in nonequilibrium lattice systems, Rev. Mod. Phys. **76**, 663–724 (2004).
[13] S. Lübeck, Universal scaling behavior of non-equilibrium phase transitions, Int. J. Mod. Phys. **18**, 3977–4118 (2004).
[14] H. Hinrichsen, Non-equilibrium critical phenomena and phase transitions into absorbing states, Adv. Phys. **49**, 815–958 (2000).
[15] D. Stauffer and A. Aharony, *Introduction to Percolation Theory*, Taylor & Francis, London, 1992.
[16] I. Jensen, Low-density series expansions for directed percolation: III. Some two-dimensional lattices, J. Phys. **A 37**, 6899–6915 (2004).
[17] E. Domany and W. Kinzel, Equivalence of cellular automata to Ising models and directed percolation, Phys. Rev. Lett. **53**, 311–314 (1984).
[18] W. Kinzel, Phase transitions of cellular automata, Z. Phys. **B 58**, 229–244 (1985).
[19] S. Wolfram, Statistical mechanics of cellular automata, Rev. Mod. Phys. **55**, 601–644 (1983).
[20] G. F. Zebende and T. J. P. Penna, The Domany-Kinzel cellular automaton phase diagram, J. Stat. Phys. **74**, 1273–1279 (1994).
[21] I. Dornic, H. Chaté, J. Chave, and H. Hinrichsen, Critical coarsening without surface tension: the voter universality class, Phys. Rev. Lett. **87**, 5701–5704 (2001).
[22] T. E. Harris, Contact interactions on a lattice, Ann. Prob. **2**, 969 (1974).
[23] R. Dickman and J. K. da Silva, Moment ratios for absorbing-state phase transitions, Phys. Rev. **E 58**, 4266–4270 (1998).
[24] J. F. F. Mendes, R. Dickman, M. Henkel, and M. C. Marques, Generalized scaling for models with multiple absorbing states, J. Phys. **A 27**, 3019–3028 (1994).
[25] H. K. Janssen, On the nonequilibrium phase transition in reaction-diffusion systems with an absorbing stationary state, Z. Phys. **B 42**, 151–154 (1981).
[26] P. Grassberger, On phase transitions in Schlögl's second model, Z. Phys. **B 47**, 365–374 (1982).
[27] H. K. Janssen and U. C. Täuber, The field theory approach to percolation processes, Ann. Phys. (N.Y.) **315**, 147–192 (2005).
[28] U. C. Täuber, M. J. Howard, and B. P. Vollmayr-Lee, Applications of field-theoretic renormalization group methods to reaction-diffusion problems, J. Phys. **A 38**, R79–R131 (2005).
[29] R. Rammal, C. Tannous, and P. Brenton, Flicker (1/f) noise in percolation networks: A new hierarchy of exponents, Phys. Rev. Lett. **54**, 1718–1721 (1985).
[30] L. de Arcangelis, S. Redner, and A. Coniglio, Anomalous voltage distribution of random resistor networks and a new model for the backbone at the percolation threshold, Phys. Rev. B **31**, 4725–4727 (1985).
[31] O. Stenull and H. K. Janssen, Transport on directed percolation clusters, Phys. Rev. E **63**, 025103 (2001).
[32] H. Hinrichsen, O. Stenull, and H. K. Janssen, Multifractal current distribution in random-diode networks, Phys. Rev. E **65**, 045104–045107 (2002).

[33] C. N. Yang and T. D. Lee, Statistical theory of equations of state and phase transitions: 1. Theory of condensation, Phys. Rev. E **87**, 404–409 (1952).
[34] C. N. Yang and T. D. Lee, Statistical theory of equations of state and phase transitions: 2. Lattice gas and Ising model, Phys. Rev. E **87**, 420–419 (1952).
[35] B. Derrida, L. de Seeze, and C. Itzykson, Fractal structure of zeros in hierarchical models, J. Stat. Phys. **33**, 559–569 (1983).
[36] P. F. Arndt, Yang-Lee theory for a nonequilibrium phase transition, Phys. Rev. Lett. **84**, 814–817 (2000).
[37] S. M. Dammer, S. R. Dahmen, and H. Hinrichsen, Yang-Lee zeros for a nonequilibrium phase transition, J. Phys. **A 35**, 4527–4539 (2002).
[38] D. Zhong and D. ben Avraham, Universality class of two-offspring branching annihilating random walks, Phys. Lett. **A 209**, 333–337 (1995).
[39] J. Cardy and U. C. Täuber, Theory of branching and annihilating random walks, Phys. Rev. Lett. **77**, 4780 (1996).
[40] J. Cardy and U. C. Täuber, Field theory of branching and annihilating random walks, J. Stat. Phys. **90**, 1–56 (1998).
[41] J. T. Cox and D. Griffeath, Diffusive clustering in the two-dimensional voter model, Annals of Probability **14**, 347–370 (1986).
[42] M. Scheucher and H. Spohn, A soluble kinetic model for spinodal decomposition, J. Stat. Phys. **53**, 279–294 (1988).
[43] L. Frachebourg and P. L. Krapivsky, Exact results for kinetics of catalytic reactions, Phys. Rev. E **53**, R3009–R3012 (1996).
[44] O. A. Hammal, H. Chaté, I. Dornic, and M. A. Muñoz, Langevin description of critical phenomena with two symmetric absorbing states, Phys. Rev. Lett. **94**, 230601–230604 (2005).
[45] M. Rossi, R. Pastor-Satorras, and A. Vespignani, Universality class of absorbing phase transitions with a conserved field, Phys. Rev. Lett. **85**, 1803–1806 (2000).
[46] S. S. Manna, Two-state model of self-organized criticality, J. Phys. **A 24**, L363 (1991).
[47] M. Henkel and H. Hinrichsen, The non-equilibrium phase transition of the pair-contact process with diffusion, J. Phys. **A 37**, R117–R159 (2004).
[48] P. Grassberger, On phase transitions in Schlög's second model, **47**, 365 (1982).
[49] M. J. Howard and U. C. Täuber, 'Real' versus 'imaginary' noise in diffusion-limited reactions, J. Phys. **A 30**, 7721 (1997).
[50] E. Carlon, M. Henkel, and U. Schollwöck, Critical properties of the reaction-diffusion model $2A \to 3A$, $2A \to \emptyset$, Phys. Rev. E **63**, 036101 (2001).
[51] J. Kockelkoren and H. Chaté, Absorbing phase transition of branching-annihilating random walks, Phys. Rev. Lett. **90**, 125701 (2003).
[52] G. Ódor, Critical behaviour of the one-dimensional annihilation-fission process $2A \to \emptyset$, $2A \to 3A$, Phys. Rev. E **62**, R3027 (2000).
[53] G. Ódor, Critical behaviour of the one-dimensional diffusive pair-contact process, Phys. Rev. E **67**, 016111 (2003).
[54] M. Paessens and G. M. Schütz, Phase transitions and correlations in the bosonic pair contact process with diffusion: exact results, J. Phys. **A 37**, 4709–4722 (2004).
[55] H. Hinrichsen, Cyclically coupled spreading and pair-annihilation, **291**, 275 (2001).
[56] J. D. Noh and H. Park, Novel universality class of absorbing transitions with continuously varying exponents, Phys. Rev. E **69**, 016122 (2004).
[57] R. Dickman and M. A. F. de Menezes, Nonuniversality in the pair-contact process with diffusion, Phys. Rev. E **66**, 045101 (2002).
[58] H. Hinrichsen, Stochastic cellular automaton for the coagulation-fission process $2A \to 3A$, $2A \to A$, **320**, 249 (2003).
[59] G. T. Barkema and E. Carlon, Universality in the pair-contact process with diffusion, Phys. Rev. E **68**, 036113 (2003).

[60] H. Hinrichsen, The diffusive pair-contact process and non-equilibrium wetting, 2003, unpublished notes, `cond-mat/0302381`.

[61] J. L. Cardy and P. Grassberger, Epidemic models and percolation, J. Phys. **A 18**, L267–L271 (1985).

[62] A. Jimenez-Dalmaroni and H. Hinrichsen, Epidemic spreading with immunization, Phys. Rev. E **68**, 036103–036114 (2003).

[63] S. M. Dammer and H. Hinrichsen, Epidemic spreading with immunization and mutations, Phys. Rev. E **68**, 016114–016121 (2003).

[64] L. Hufnagel, D. Brockmann, and T. Geisel, Forecast and control of epidemics in a globalized world, Proc. Nat. Acam. Sci. **101**, 15124–15129 (2004).

[65] D. Brockmann, L. Hufnagel, and T. Geisel, Human dispersal on geographical scales, 2005, preprint, submitted.

[66] D. Mollison, Spatial contact models for ecological and epidemic spread, J. Roy. Stat. Soc. **B 39**, 283 (1977).

[67] J.-P. Bouchaud and A. Georges, Anomalous diffusion in disordered media: statistical mechanics, models and physical applications, Phys. Rep. **195**, 127–293 (1990).

[68] H. C. Fogedby, Langevin equations for continuous Lévy flights, Phys. Rev. E **50**, 1657–1660 (1994).

[69] P. Grassberger, in *Fractals in physics*, edited by L. Pietronero and E. Tosatti, Elsevier, Amsterdam, 1986.

[70] M. C. Marques and A. L. Ferreira, Critical behaviour of a long-range non-equilibrium system, J. Phys. **A 27**, 3389–3395 (19).

[71] E. V. Albano, Branching annihilating Lévy flights: Irreversible phase transitions with long-range interactions, Europhys. Lett. **34**, 97–102 (1996).

[72] H. K. Janssen, K. Oerding, F. van Wijland, and H. J. Hilhorst, Lévy-flight spreading of epidemic processes leading to percolating clusters, Euro. Phys. J. **B 7**, 137–145 (1999).

[73] H. Hinrichsen and M. Howard, A model for anomalous directed percolation, Euro. Phys. J. **B 7**, 635–643 (1999).

[74] A. Jimenez-Dalmaroni and J. Cardy, 2005, in preparation.

[75] J. Adamek, M. Keller, A. Senftleben, and H. Hinrichsen, Epidemic spreading with long-range infections and incubation times, J. Stat. Mech. , to appear (2005).

[76] S. Dietrich, Wetting phenomena, in *Phase transitions and critical phenomena*, edited by C. Domb and J. L. Lebowitz, volume 12, Academic Press, London, 1988.

[77] G. P. M. Kardar and Y.-C. Zhang, Dynamic scaling of growing interfaces, Phys. Rev. Lett. **56**, 889–892 (1986).

[78] Y. Tu, G. Grinstein, and M. A. Muñoz, Systems with multiplicative noise: critical behavior from KPZ equation and numerics, Phys. Rev. Lett. **78**, 274–277 (1997).

[79] M. A. Muñoz and T. Hwa, On nonlinear diffusion with multiplicative noise, Europhys. Lett. **41**, 147–152 (1998).

[80] U. Alon, M. R. Evans, H. Hinrichsen, and D. Mukamel, Roughening transition in a one-dimensional growth process, Phys. Rev. Lett. **76**, 2746–2749 (1996).

[81] U. Alon, M. Evans, H. Hinrichsen, and D. Mukamel, Smooth phases, roughening transitions, and novel exponents in one-dimensional growth models, Phys. Rev. **E 57**, 4997–5012 (1998).

[82] H. Hinrichsen, R. Livi, D. Mukamel, and A. Politi, A model for nonequilibrium wetting transitions in two dimensions, Phys. Rev. Lett. **79**, 2710–2713 (1997).

[83] H. Hinrichsen, R. Livi, D. Mukamel, and A. Politi, First order phase transition in a 1+1-dimensional nonequilibrium wetting process, Phys. Rev. **E 61**, R1032–R1035 (2000).

[84] H. Hinrichsen, R. Livi, D. Mukamel, and A. Politi, Wetting under non-equilibrium conditions, Phys. Rev. E **68**, 041606 (2003).

[85] H. Hinrichsen, On possible experimental realizations of directed percolation, Braz. J. Phys. **30**, 69–82 (2000).